Chapter 17
Fabrication of Micro-structured Polymer Via Precision Grinding and Injection Molding

Yanjun Lu, Xingyu Mou, and Fumin Chen

Abstract In this chapter, precise micro-grinding machining was proposed to create regular and controllable micro-grooved array structures on the surface of mold cores for the mass production and fabrication of micro-structured polymer components by micro injection molding. First, the 3D topology and cross-sectional profiles of a micro-ground mold cores and micro-formed polymer with various microstructural parameters are presented. The surface roughness of the mold cores and polymers is then compared. Secondly, the relationship between the accuracy of the microbead-treated mould core and the fillability of the micro-structured injection polymer is investigated. Finally, the effect of micro injection molding parameters on the filling rate of micro-structures polymer were investigated. The results show that micro-structured polymers can be produced efficiently and rapidly using the proposed method. The experimental results show that the highest shape accuracy and filler level of the micro-structured polymer can be achieved at 4.05 μm and 99.30% respectively for a mold core with micro-grooves. It was found that the degree of filling of the micro-structured polymer increased approximately with the accuracy of the core processing. Injection pressure has the greatest influence on the degree of filling of the molded polymer, while melt temperature has the least effect.

1 Introduction

Micro-structured polymer devices have been applied in many fields such as optical, biomedical, electronic and microelectro-mechanical systems (MEMS) [1–3]. Currently, the main microforming techniques for micro-structured polymers are microinjection molding, microthermal compression molding, and injection and pressure molding [4, 5]. Microinjection molding has become an alternative method for mass production and fabrication of micro-structured polymer products due to its short

Y. Lu (✉) · X. Mou · F. Chen
Guangdong Provincial Key Laboratory of Micro/Nano Optomechatronics Engineering, College of Mechatronics and Control Engineering, Shenzhen University, Nan-Hai Ave 3688, Shenzhen 518060, Guangdong, PR China
e-mail: luyanjun@szu.edu.cn

G. Zhang et al. (eds.), *Fabrication of Micro/Nano Structures via Precision Machining*,
https://doi.org/10.1007/978-981-99-1338-1_17

molding cycle time, high efficiency, and low production cost [6, 7]. For example, superhydrophobic polymer surfaces with a layered structure of micro- and nano-cylinders have been successfully produced by microinjection molding [8]. It has been shown that droplets on layered micro- and nanopolymer surfaces reach a contact angle of about 163°, which gives them self-cleaning properties. An amorphous polymer surface with a high aspect ratio microstructure was fabricated by microinjection molding for erythrocyte depletion in bioelectromechanical systems [9]. The temperature of the mold proved to have the greatest influence on the degree of replication of microfeatures compared to other major process parameters. Microinjection molding has been used to produce microinjected polymer surfaces by replicating the microscopic features of molded inserts with microcavity structures [10]. Experimental results have shown that small cavity thickness and high mold temperature have a positive influence on the level of replication of micro features.

However, high-precision machining of the mold core surface to produce micro-nanostructures is very difficult, which directly determines the quality of micro-forming of micro-structured polymer products. Many advanced processing techniques have emerged for microscale machining of mold core microstructure surfaces, such as chemical etching [11], laser processing [12], electrical discharge machining (EDM) [13], and fluid jet array parallel machining (FJAPM) [14]. Although chemical etching and laser processing techniques can produce nanoscale microtextured structures, they are difficult to use to ensure the accuracy of the three-dimensional morphology of micron-scale microstructures. Although electrical discharge machining (EDM) can effectively fabricate complex 3D microstructures, it is difficult to achieve smooth microstructure surfaces. Parallel processing using fluid jet arrays (FJAPM) can produce smooth microstructure surfaces, but requires significant processing time. It was found that a dressed superhard diamond grinding wheel can perform precision micromachining of wire drawing mold cores to obtain smooth micro-structured surfaces [15–17]. To achieve high shape accuracy and surface quality of microstructures in the micron range, this study proposes an efficient and precise micro–ground technique to produce micron-sized slotted mesh structures with controlled shape accuracy on the mold core surface. In addition, the micro–ground process is very simple and the production cost is relatively low.

In this chapter, the regular and controlled micro-grooved array structures on the surface of mold core were machined by micro-grinding machining with a trued V-tip diamond grinding wheel. Micro injection molding technology rapidly produces micro-structured polymer parts by replicating microscopic features on the surface of the mold core. The surface morphology and V-groove profile of mold cores and micro-structured polymers are presented, and the shape accuracy of micro-grinding and the filling degree of micro-injection molding are analyzed. The surface roughness of the micro-ground mold cores and the micro-formed polymers are compared. In addition, the relationship between the shape accuracy of the micro-ground core and the degree of filling of the micro-structured polymer was revealed. The effect of microinjection molding parameters on the degree of filling of micro-structured polymers was also analyzed.

2 Materials and Methods

2.1 Micro-grinding of Mold Core with V-Grooved Array Structures

Titanium carbide (Ti_3SiC_2) has both metallic and ceramic properties, which is compared to conventional mold core materials, such as excellent machinability, good electrical conductivity, high wear resistance and good self-lubrication [18, 19]. In this experiment, Ti_3SiC_2 ceramic was chosen as the mold core material because of its good lubrication and self-lubrication properties.

Figure 1 shows a schematic diagram and photographs of microfabrication of the V-groove structure on the Ti_3SiC_2 mold core surface using a computer-controlled precision grinder (CNC). First, the V-groove grinding head of the diamond wheel was mechanically ground using a CNC interpolation path [20] to straighten it out. The Ti_3SiC_2 ceramic substrate was then installed on the horizontal table of the grinding machine. The machined V-shaped diamond wheel is driven by the CNC for grinding the Ti_3SiC_2 tool core (see Fig. 1a). By mimicking the V-shape of the diamond wheel, V-grooves are gradually formed on the surface of the Ti_3SiC_2 core. When one V-groove is completed, the diamond wheel is moved in the specified space in the Z-axis direction to carry out the grinding process for the second V-groove. Finally, a micro-groove structure is formed on the surface of the toolholder according to the specified machining path. Figure 1b shows a picture of the machining of the mold core. As Ti_3SiC_2 is a ceramic material, the conditions for micro-grinding the mold core with a V-shaped diamond wheel were chosen based on previous machining experience (see Table 1). Six sets of well-developed V-grooves were ground on the surface of the substrate core under the same grinding conditions. The V-groove parameters developed include the V-groove angle α, the V-groove depth h and the V-groove space b, as shown in Table 2. The corresponding mold cores with various V-grooved array structures are called as A_m, B_m, C_m, D_m, E_m and F_m sections respectively.

2.2 Micro Injection Molding of Micro-structured Polymers

With the micro injection molding machine (Babyplast 6/10P, Cronoplast Sl, Barcelona, Spain), the V-groove array structure of the mold core surface can be reproduced on the part surface, as shown in Fig. 2a. With its metal ball plasticizing system and piston injection system, this efficient and precise micro injection molding machine is ideal for mass production and processing of all thermoplastic micro precision parts. Figure 2b shows the operation of the micro injection molding machine. For this experiment, polypropylene (PP) pellets (B310, Lotte Chemical Corporation, Seoul, Korea) were selected as the material for the polymer part and placed in the hopper. The flow rate, density, heat deflection temperature and melting point of the polymer material were 0.5 g/10 min, 0.9 g/cm^3, 110 °C and 167 °C, respectively. The

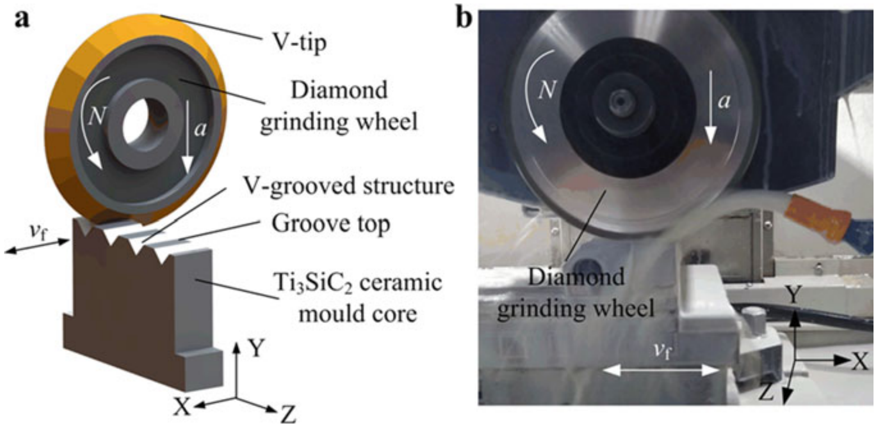

Fig. 1 Micro-grinding machining scheme and image of mold core: **a** Schematic diagram of V-grooved structures machining; **b** Image of micro-grinding

Table 1 Micro-grinding conditions of mold core using a V-tip diamond grinding wheel

CNC grinder	SMART B818 III
Diamond grinding wheel	SD3000, resin bond, diameter D = 150 mm, width B = 4 mm, Wheel speed N = 3000 r/min
Workpiece	Ti_3SiC_2 ceramic mold core
Rough machining	Feed speed $v_f = 1000$ mm/min, depth of cut $a = 5$ μm
Finish machining	Feed speed $v_f = 100$ mm/min, depth of cut $a = 1$, $\Sigma a = 10$ μm
Coolant	Emulsion

Table 2 The designed V-grooved structure parameters of mold cores

Sample	V-groove angle α (°)	V-groove depth h (μm)	V-groove space b (μm)
A_m	90	100	400
B_m	90	100	500
C_m	90	100	600
D_m	90	150	400
E_m	90	150	500
F_m	90	150	600

counter mold has a core shape with a V-grooved array structure. Polymer particles are first heated and plasticized, then melted by an electric piston and injected into the front cavity of the mold through a nozzle. The cavity is then cooled while maintaining a certain pressure. Finally, the micro-structured polymer is produced when the front and back side of the mold are simultaneously demolded.

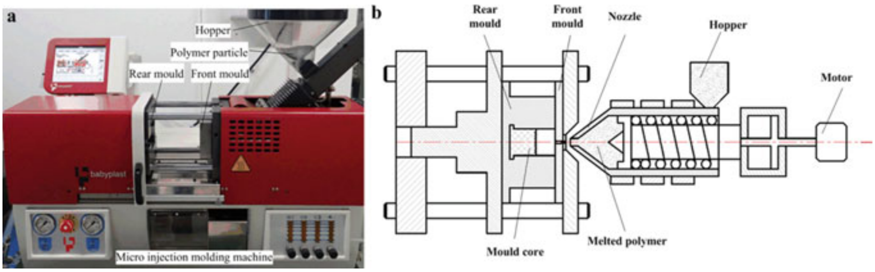

Fig. 2 Photograph and working principle of the micro injection molding machine: **a** photograph; **b** working principle

Figure 3 shows a sketch of the mold frame and mold core design. Figure 3a shows the whole mold frame. Figure 3b shows a schematic of the front side of the mold. The polymer material which is melted and plasticized is injected into the front mold cavity through the pouring port. Figure 3c shows a schematic view of the rear mold, which is equipped with a core. Figure 3d shows a schematic view of a mold core with V-grooves obtained by microfabrication.

Figure 4 shows the microinjection molding process of a micro-structured polymer. The V-groove of the mold core is repeated on the polymer surface to create an inverted V-groove structure after micro injection molding. The V-groove parameters of the micro-ground mold core are characterized as V-groove angle α_1, V-groove depth h_1 and V-groove space b_1. The V-groove parameters of the micro-structured polymer are characterized as V-groove angle α_2, V-groove depth h_2 and V-groove space b_2. The surface quality of the micro-structured polymer at the edge of the groove and at the bottom of the groove depends on the quality of the groove edge and the quality of the top edge of the core groove. Under the same conditions, six sets of micro-ground mold cores were used for micro-injection experiments. According to the preliminary tests, the melting temperature was set at 210 °C, the injection speed was 40 mm/s, the injection speed was 7 MPa, and the holding pressure and pressure retention time were 5 s. After microinjection molding, the corresponding micro-structured polymer samples were defined as A_w, B_w, C_w, D_w, E_w and F_w.

In order to investigate the effects of melt temperature T, injection rate v, injection pressure P and residence time t on the degree of filling of micro-structured polymers, the experimental parameters listed in Table 3 were developed. Thirty micro-structured polymer samples were prepared under each process parameter condition, and five random samples were selected for testing and averaging.

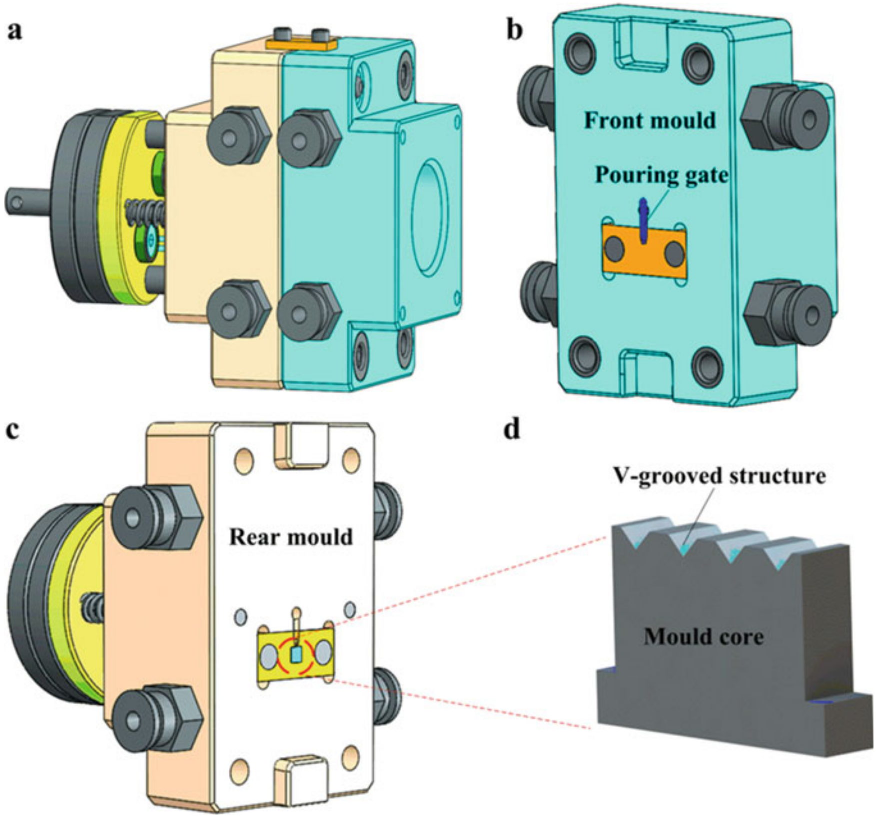

Fig. 3 The design sketches of mold frame and mold core: **a** the whole mold frame; **b** the front mold; **c** the rear mold; **d** the mold core

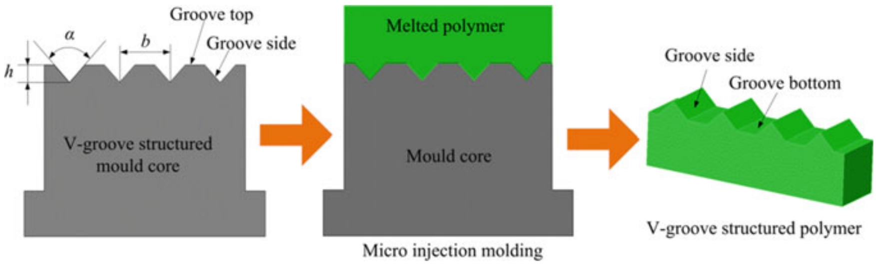

Fig. 4 Principle of micro injection molding of the micro-structured polymer

Table 3 Experimental parameter lists of micro injection molding

No	Melt temperature T (°C)	Injection speed v (mm/s)	Injection pressure P (MPa)	Holding time t (s)
1	200	40	7	3
2	205	40	7	3
3	210	40	7	3
4	215	40	7	3
5	220	40	7	3
6	210	30	7	3
7	210	35	7	3
8	210	45	7	3
9	210	50	7	3
10	210	40	5	3
11	210	40	6	3
12	210	40	8	3
13	210	40	9	3
14	210	40	7	1
15	210	40	7	2
16	210	40	7	4
17	210	40	7	5

2.3 Measurement of Micro-grooved Mold Cores and Polymers

High-resolution scanning electron microscopy (SEM, FEI Quanta 450FEG and Apreo S, FEI Corporation, Hillsboro, OR, USA) was used to research the surface morphology of micro-structured mold cores. A 3D laser scanning microscope (VK-250, Keyence, Osaka, Japan) was used to measure the 3D morphology and cross-sectional profile of the micro-structured form bars. A probe stepper (D-300, KLA-Tencor, Milpitas, CA, USA) was used to measure the cross-sectional profile of the micro-structured polymer. Using data analysis software, the cross-sectional profiles were used to determine the surface roughness and V-curvature angle. The results presented are the average of five measurements.

3 Results and Discussions

3.1 Surface Topographies and Profiles of Micro-ground Mold Core

Figure 5 shows the 3D topographies and section profiles of the mold core with micro-grooved array structures after micro-grinding. It can be seen from the figure that a regular and uniform V-groove array structure is completely created on the surface of the mold core. The parameters of the micromachined V-groove structure are given in Table 4, which are approximately the same as those given in Table 2. the V-groove angle α was obtained from the V-groove profile measured by a 3D laser scanning microscope. the angular error of the V-shaped micro-grooves varied from 0.88 to 1.87°, with an average angular error of 1.38°. The average errors of micro-groove depth and V-groove spacing were 2.62 μm and 2.73 μm, respectively. The actual distance of the V-groove in the cast bar was slightly larger than the theoretical value, which was mainly influenced by the non-circular surface of the diamond grinding wheel.

Figure 6 shows an SEM photograph of the surface of the micro-ground mold core. the SEM observation shows that the morphological characteristics of the V-groove surface are generally consistent with the 3D morphological measurements in Fig. 5. It can also be found that the surface on one side of the V-groove is smoother than the surface above the groove (the unground surface). The surface of the V-groove of sample D_m is the smoothest and most uniform compared to the other samples.

3.2 Surface Topographies and Profiles of Micro-structured Polymers

Figure 7 shows the SEM topography of the micro-structured polymer after microinjection molding. It can be found from the SEM image that the V-shaped structure of the mold core is preferentially repeated on the polymer, forming an inverted V-shaped structure. It can be seen that the surface of the D_w microstructure is the smoothest, with a roughness Ra of 0.052 μm on the groove side. It can also be found that the V-groove side of the microinjected polymer is smoother than the V-groove side of the mold core (see Figs. 6d and 7d). The microinjected surfaces of samples B_w, C_w and F_w show many cracks and melted polymer. This was attributed to the poor quality of the bead blasted surfaces of the respective mold sticks, which led to difficulties in demolding during the microinjection process. For all the micro-formed polymers, the sides of the V-groove were smoother than the bottom of the V-groove. This is due to the fact that the surface quality of the bottom of the polymer groove depends on the unpolished top surface of the mold core groove.

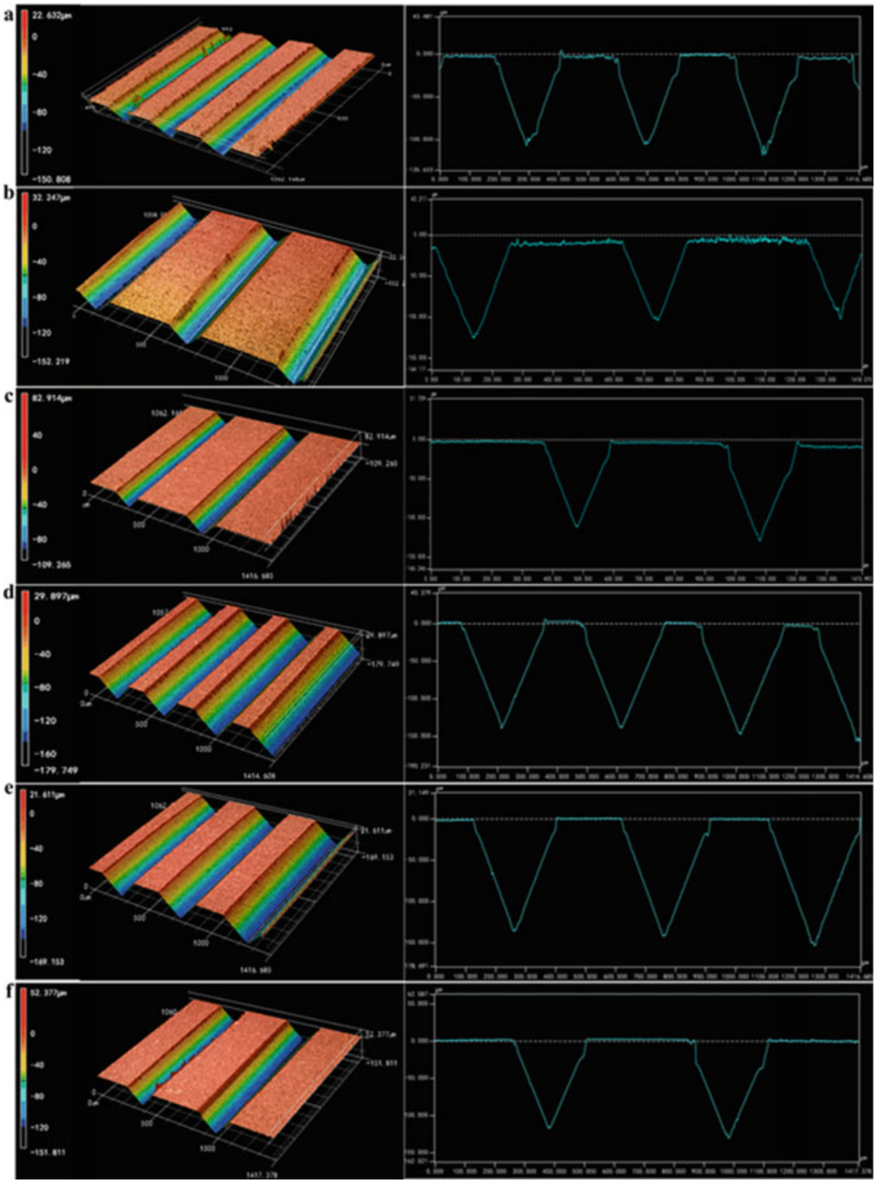

Fig. 5 3D topographies and profiles of micro-ground mold cores: **a** Sample A_m; **b** Sample B_m; **c** Sample C_m; **d** Sample D_m; **e** Sample E_m; **f** Sample F_m

Table 4 The V-grooved structure parameters of micro-ground mold cores

Sample	V-groove angle α_1 (°)	V-groove depth h_1 (μm)	V-groove space b_1 (μm)
A_m	90.88	99.72	400.43
B_m	91.87	106.64	503.17
C_m	91.80	100.37	604.17
D_m	91.17	148.10	401.97
E_m	91.19	152.61	506.52
F_m	91.35	153.93	599.86

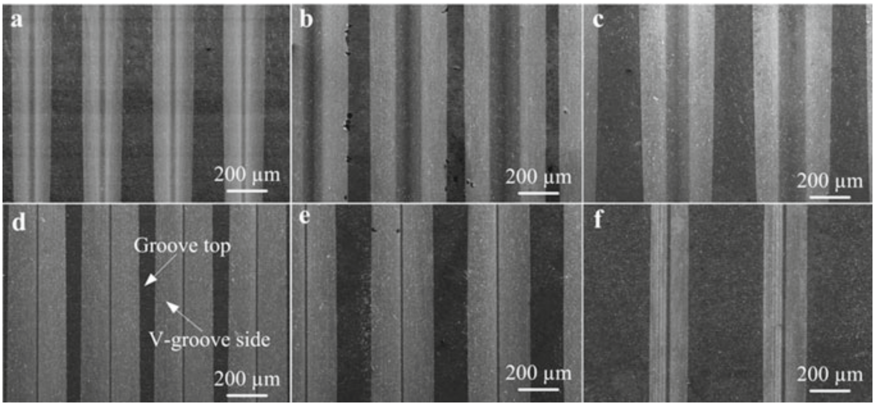

Fig. 6 SEM photographs of micro-ground mold cores: **a** Sample A_m; **b** Sample B_m; **c** Sample C_m; **d** Sample D_m; **e** Sample E_m; **f** Sample F_m

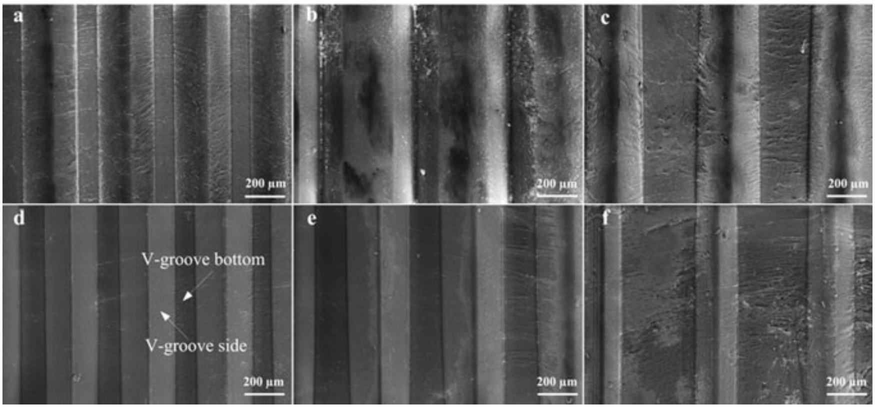

Fig. 7 SEM photographs of micro-structured polymers: **a** Sample A_w; **b** Sample B_w; **c** Sample C_w; **d** Sample D_w; **e** Sample E_w; **f** Sample F_w

Since the polymer is nonopaque, the cross-sectional profile of the micro-structured polymer surface is recorded using a contact profiler. Figure 8 shows the cross-sectional profile of the V-groove of the micro-structured polymer after micro injection molding. Table 5 shows the structural parameters of the V-groove polymer. The V-groove profile is circular due to the core radius of the V-groove shape and the diamond grinding wheel used for grinding. Compared to the calculated V-groove parameters shown in Table 2, the angular error on the micro-structured polymer surface of the V-groove ranged from 0.02 to 0.88° with an average angular error of only 0.46°. The average micromachining depth of the V-groove was 2.42 μm with a spatial error of 1.12 μm. The D_w sample showed the highest micromachining accuracy compared to the V-groove profile. This result also agrees with the SEM image shown in Fig. 7.

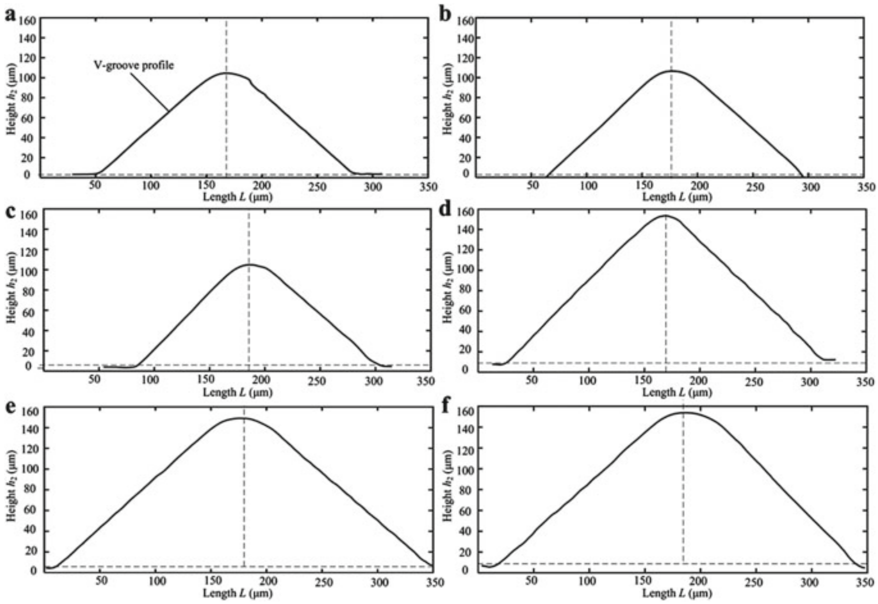

Fig. 8 The profiles of micro-structured polymers: **a** Sample A_w; **b** Sample B_w; **c** Sample C_w; **d** Sample D_w; **e** Sample E_w; **f** Sample F_w

Table 5 The V-grooved structure parameters of micro-structured polymers

Sample	V-groove angle α_2 (°)	V-groove depth h_2 (μm)	V-groove space b_2 (μm)
A_w	89.98	98.74	400.40
B_w	89.98	106.50	500.40
C_w	89.12	98.43	600.50
D_w	90.81	147.15	398.00
E_w	89.26	150.77	501.40
F_w	90.26	151.55	598.00

3.3 Machining Accuracy of Micro-ground Mold Core and Filling Rate of Micro-formed Polymer

Although the equipment used to measure the contours of the mold core and the polymer are different, the experience gained so far using both devices shows that the results are essentially the same. By comparing the contours of the V-groove of the mold core and the micro-tip of the grinding wheel tool, it can obtain the contour error distribution and the angular error profile. The profile error e_m is defined as the height difference between the V-groove profile of the mold core and the microtip profile of the diamond grinding wheel. The relative angular error α_m of the V-groove of the mold core can be calculated according to the following equation:

$$\alpha_m = \frac{|\alpha - \alpha_1|}{\alpha} \times 100\% \tag{1}$$

where α is the V-groove angle of the wheel tool tip and α_1 is the V-groove angle of micro-structured mold core. Due to the offset of the end face of the diamond grinding wheel, the V-tip angle of mold core surface was commonly larger than that of the wheel tool tip. The morphological accuracy γ of the mold core can be defined as the difference between the tip and the valley of the contour error curve [21].

Figure 9 shows the relative angular error α_m and the shape accuracy γ of the mold core. Based on the curves of the V-groove profile of mold core and wheel tool tip which is shown in Fig. 9a, the distribution curve for mold defects in the mold core can be determined as shown in Fig. 9b. It shows that the largest shape defect occurs at the tip of the V-groove. This is because the tip of the micromachined V-groove has been a technical bottleneck, so the radius of the circle has been present. It turns out that the contour error of the V-tip can be controlled to within 5 μm using the micro-sharpened mold core. Figure 9c shows the relative angular error α_m for all mold cores, which ranged between 1.0 and 2.1%. The average relative angular error of the finely ground cores is only 1.53%. The shape accuracy γ is determined by the shape error distribution curve shown in Fig. 9b. Figure 9d shows that the lowest shape accuracy of 4.05 μm is obtained for the molded core D_m. The micro-grinding accuracy is below 10 μm for all types of cores except for the B_m and C_m type cores.

By comparing the profile of the V-groove with the profile of the mold core and the polymer, the profile defect distribution and the angular defect can be determined. Thus, the relative defect α_w of the V-groove angle of the polymer can be calculated as follows:

$$\alpha_w = \frac{|\alpha_1 - \alpha_2|}{\alpha_1} \times 100\% \tag{2}$$

where α_2 is the V-groove angle of the micro-structured polymer. The filling ratio η of injection molding can be calculated according to the following equation:

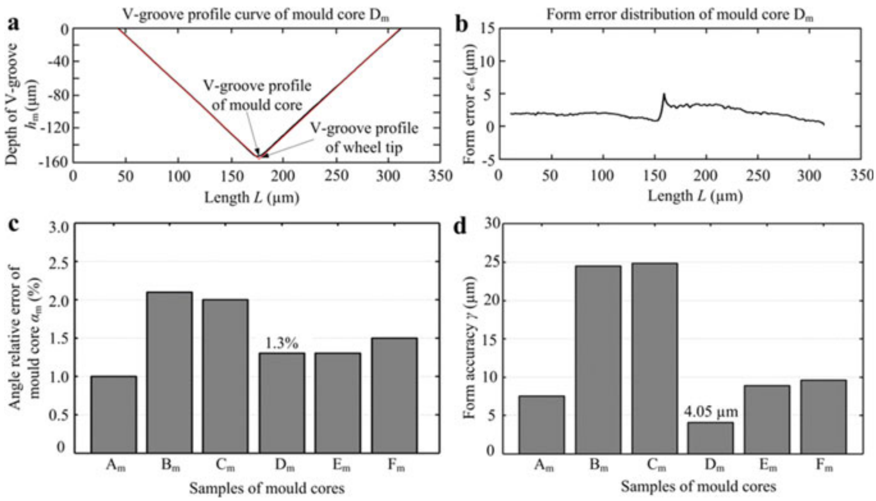

Fig. 9 The angle relative error α_m and form accuracy γ of mold core: **a** V-groove profile curves of wheel tip and mold core D_m; **b** form error distribution of mold core D_m; **c** angle relative error α_m; **d** form accuracy γ

$$\eta = 1 - \frac{1}{N}\sum\frac{|h_1 - h_2|}{h_1} \times 100\% \tag{3}$$

where h_1 is the V-groove depth value of the mold core, h_2 is the V-groove depth of the polymer workpiece, and N is the data point of the measured V-groove profile.

Figure 10 shows the relative angular error α_w and the filling factor η for the micro-structured polymers. Figure 10c shows the relative angular error α_w for all micro-structured polymers, which ranges from 0.4 to 2.9%. The average relative angular error of the micro-structured polymers is only 1.58%. The results show that D_w polymers have the lowest relative angular error of 0.4%. It was also found that the V-vertex of the micro-structured polymers.

The angle was smaller than the V-groove angle of the mold core. The reason is that the shrinkage of the injection molded polypropylene (PP) during the cooling process, which leads to the reduction of the V-groove angle. As can be seen from Fig. 10c, the larger the space of the V-groove, the larger the relative angle error. The reason for this may be that the larger the space of the V-groove, the faster the micro-formed polymer shrinks, leading to a rise in the V-groove angle. Figure 10d shows the degree of filling η for all micro-structured polymers. it can be found that the blank D_w has the highest degree of filling with 99.30%. By comparing with Figs. 9d and 10d, it can be concluded that the higher the mold accuracy of the core processing, the higher the degree of filling of the micro-structured polymer. It was also found that the greater the depth or depth-to-width ratio of the V-groove, the higher the filling rate.

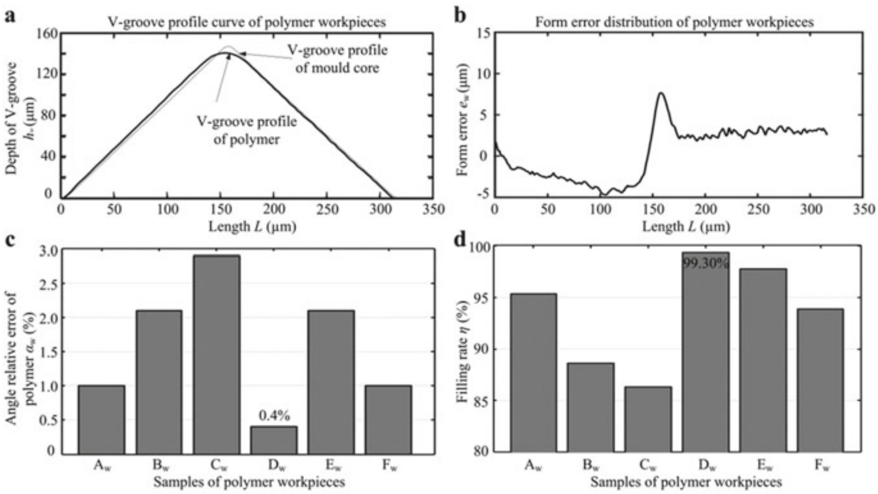

Fig. 10 The angle relative error α_W and filling rate η of micro-structured polymer: **a** V-groove profile curves of polymer D_W and mold core D_m; **b** form error distribution of polymer D_W; **c** angle relative errors α_W; **d** filling rates η

3.4 Surface Quality Analysis of Mold Core and Injection Molded Polymers

Based on the micro-forming principle of micro-structured polymers in microinjection molding, the surface roughness of the polymer on the side of the groove and the bottom of the groove depend on the side of the micro-ground groove and the top of the unground core groove, respectively, as shown in Fig. 4. Figure 11a shows the surface roughness Ra on the side of the mold core and polymer groove. Figure 11b shows a comparison of the surface roughness Ra on the top side of the mold core groove and the bottom side of the polymer groove. It can be seen that the surface roughness Ra of the groove sides of the micro-ground mold core and the micro-formed polymer are in the range of 0.271–0.336 μm and 0.052–0.092 μm, respectively, which indicates that the surface quality of the molded polymer is better than the quality of the molded core. The surface roughness Ra on the groove side of the microporous core Dm was the lowest at 0.271 μm, while the corresponding polymer D_w reached the lowest value of 0.052 μm. The surface roughness Ra on the groove side of the micro-ground polymer remained below 0.1 μm. It was also shown that the upper surface of the grooves of the cast core was unpolished and much rougher than the surface of the micro-formed grooves, which resulted in a poorer surface quality at the bottom of the grooves of the micro-structured polymers.

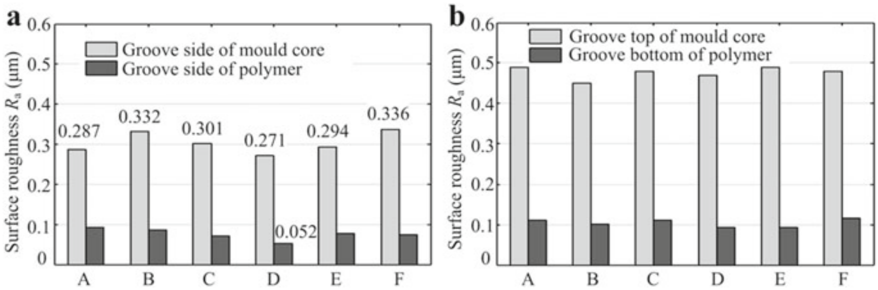

Fig. 11 Comparisons of surface roughness R_a of micro-structured mold cores and polymers: **a** groove sides of mold core and polymer; **b** groove top of mold core and groove bottom of the polymer

3.5 Relationship Between the Filling Ratio of Micro-structured Polymer and the Form Accuracy of Micro-ground Mold Core

Figure 12 shows the relationship between the filling ratio η of the micro-structured polymer and the form accuracy γ of the microfine matrix rods. The form accuracies of the six matrix cores were 7.53 μm, 24.5 μm, 24.84 μm, 4.05 μm, 8.87 μm, and 9.59 μm, respectively. The corresponding fill rates of the micro-formed polymers were 86.33%, 95.34%, 88.61%, 93.85%, 97.78%, and 99.45%, respectively. The results showed that the accuracy of the mold core shape of the micro-ground mold core had a positive effect on the filling degree of microinjection molding. The degree of filling of micro-structured polymers tended to increase as the shape accuracy of the microform core decreased. This indicates that the higher the machining accuracy of the mold core, the higher the degree of filling in microinjection molding.

Fig. 12 The relationship between the filling ratio of micro-structured polymer η and form accuracy of micro-ground mold core γ

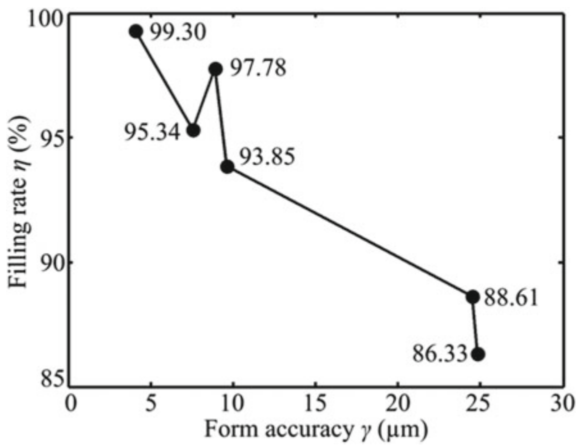

3.6 *Effects of Micro Injection Molding Parameters on the Filling Rate of Micro-structured Polymer*

As shown in Fig. 13, the filling factor η of the micro-structured polymers in relation to the microinjection parameters is presented, including melt temperature T, injection rate v, injection pressure P and residence time t. As shown in Fig. 10a, b, the filling factor η of the micro-structured polymers increased significantly with the increment of melt temperature T and injection rate v, and then decreased. The filling coefficients of micro-structured polymers were 98.25–99.30% and 92.86–99.30%, respectively. The results in Fig. 10c, d show that the filling coefficients varied between 91.19–99.30% and 92.71–99.30%, respectively, depending on the injection pressure P and residence time t. Thus, the results from experimenting indicate that the injection pressure has the dominant influence on the degree of filling of the mold polymer, while the melt temperature has the least effect. In general, the highest value of 99.30% filling of micro-structured polymers can be achieved when the melt temperature, injection velocity, injection pressure and residence time are 210 °C, 40 mm/s, 7 MPa and 5 s, respectively.

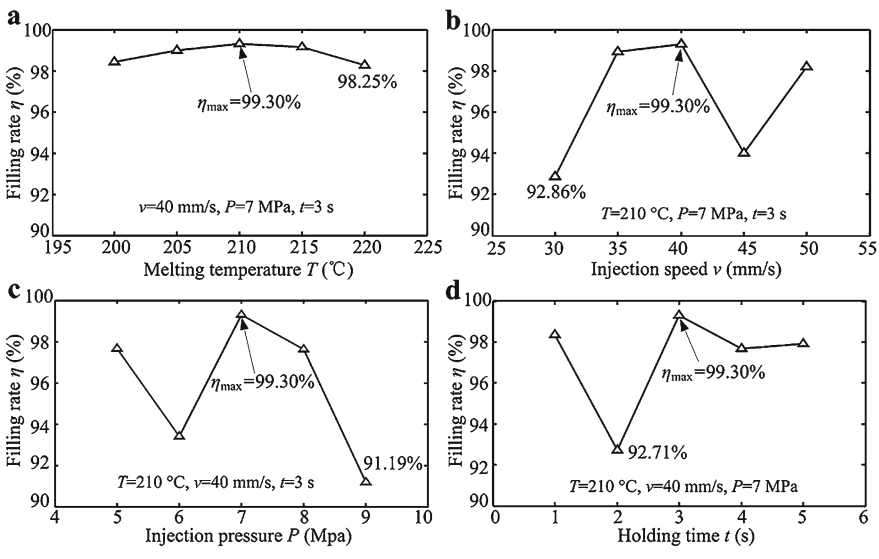

Fig. 13 The filling rate of micro-structured polymer η versus micro injection molding parameters: **a** Melting temperature T; **b** injection speed v; **c** injection pressure P; **d** holding time t

4 Conclusions

A micro-grinding method with a V-tip diamond wheel is presented to form regular and precise micro-grooved structures on the mold core surface. By micro-grinding the mold core, micro-structured polymers are produced efficiently and accurately by micro-injection molding technology. It enables cost-effective large-scale production of micro-structured polymer parts. The main results can be summarized as follows.

(1) The highest molding accuracy and filler degree of 4.05 μm and 99.30% of micro-structured polymer can be achieved by micro-milled mold cores, respectively. The minimum relative angular error of the micro-structured polymer is only 0.4%.
(2) The surface roughness R_a on the micro-structured polymer side can be as low as 0.1 μm. A minimum Ra of 0.271 microns is achieved on the core side of the micro-milled polymer, while a minimum R_a of 0.052 μm can be achieved for the corresponding micro-formed polymer.
(3) The core shape accuracy of the micro-ground mold core has a positive effect on the filling ratio of the micro-formed polymer. The fill rate of micro-formed polymers increases considerably as the shape accuracy of the core increases.
(4) Injection pressure has the dominant influence on the fill rate of micro-structured polymers. However, melt temperature has the least effect.

Acknowledgements The work described in this chapter was supported by the National Natural Science Foundation of China (Grant No. 51805334), the International Science and Technology Cooperation Project of Shenzhen City (Grant No. GJHZ20190822091805371), and the Science and Technology Planning Project of Guangdong Province (Grant No. 2017A010102003).

References

1. Maghsoudi K, Jafari R, Momen G, Farzaneh M (2017) Micro-nanostructured polymer surfaces using injection molding: a review. Mater. Today Commun 13:126–143
2. Gao S, Qiu ZJ, Ma Z, Yang YJ (2017) Development of high efficiency infrared-heating-assisted micro-injection molding for fabricating micro-needle array. Int J Adv Manuf Technol 92:831–838
3. Guarino V, Causa F, Salerno A, Ambrosio L, Netti PA (2008) Design and manufacture of microporous polymeric materials with hierarchal complex structure for biomedical application. Mater Sci Tech 24:1111–1117
4. Giboz J, Copponnex T, Mélé P (2007) Microinjection molding of thermoplastic polymers: a review. J Micromech Microeng 17:R96–R109
5. Loaldi D, Quagliotti D, Calaon M, Parenti P, Annoni M, Tosello G (2018) Manufacturing signatures of injection molding and injection compression molding for micro-structured polymer fresnel lens production. Micromachines 9:653–674
6. Bellantone V, Surace R, Trotta G, Fassi I (2013) Replication capability of micro injection molding process for polymeric parts manufacturing. Int J Adv Manuf Technol 67:1407–1421

7. Lu Z, Zhang KF (2009) Morphology and mechanical properties of polypropylene micro-arrays by micro-injection molding. Int J Adv Manuf Technol 40:490–496
8. Weng C, Wang F, Zhou MY, Yang DJ, Jiang BY (2018) Fabrication of hierarchical polymer surfaces with superhydrophobicity by injection molding from nature and function-oriented design. Appl Surf Sci 436:224–233
9. Lucchetta G, Sorgato M, Carmignato S, Savio E (2014) Investigating the technological limits of micro-injection molding in replicating high aspect ratio micro-structured surfaces. CIRP J Manuf Sci Technol 63:521–524
10. Masato D, Sorgato M, Lucchetta G (2016) Analysis of the influence of part thickness on the replication of micro-structured surfaces by injection molding. Mater. Design 95:219–224
11. Niewerth F, Necker M, Rösler J (2015) Influence of chromium on microstructure and etching behaviour of new Ni–Fe–Al based alloy. Mater Sci Tech 31:349–354
12. Zhou CL, Ngai TWL, Li LJ (2016) Wetting behaviour of laser textured Ti3SiC2 surface with micro-grooved structures. Mater Sci Tech 32:805–812
13. Debnath T, Patowari PK (2019) Fabrication of an array of micro fins using wire EDM and its parametric analysis. Mater Manuf Process 34:580–589
14. Wang CJ, Cheung CF, Liu MY, Lee WB (2017) Fluid jet-array parallel machining of optical microstructure array surfaces. Opt Express 25:22710–22725
15. Lu YJ, Xie J, Si XH (2015) Study on micro-topographical removals of diamond grain and metal bond in dry electro-contact discharge dressing of coarse diamond grinding wheel. Int J Mach Tool Manu 88:118–130
16. Zhang L, Xie J, Guo AD (2018) Study on micro-crack induced precision severing of quartz glass chips. Micromachines 9:224–238
17. Li ZP, Zhang FH, Luo XC, Guo XG, Cai YK, Chang WL, Sun JN (2018) A new grinding force model for micro grinding RB-SiC ceramic with grinding wheel topography as an input. Micromachines 9:368–386
18. Zhou CL, Wu XY, Lu YJ, Wu W, Zhao H, Li LJ (2018) Fabrication of hydrophobic Ti3SiC2 surface with micro-grooved structures by wire electrical discharge machining. Ceram Int 44:18227–18234
19. Zhou CL, Wu XY, Ngai TWL, Li LJ, Ngai SL, Chen ZM (2018) Al alloy/Ti3SiC2 composites fabricated by pressureless infiltration with melt-spun Al alloy ribbons. Ceram Int 44:6026–6032
20. Xie J, Luo MJ, Wu KK, Yang LF, Li DH (2013) Experimental study on cutting temperature and cutting force in dry turning of titanium alloy using a non-coated micro-grooved tool. Int J Mach Tool Manu 73:25–36
21. Xie J, Xie HF, Luo MJ, Tan TW, Li P (2012) Dry electro-contact discharge mutual-wear truing of micro diamond wheel V-tip for precision micro-grinding. Int J Mach Tool Manu 60:44–51